

# Identification of the Mass Donor Star's Spectrum in SS 433

T. C. Hillwig<sup>1</sup>, D. R. Gies<sup>1,2</sup>, W. Huang<sup>2</sup>, M. V. McSwain

*Center for High Angular Resolution Astronomy, Department of Physics and Astronomy,  
Georgia State University, Atlanta, GA 30303*

*thillwig@chara.gsu.edu, gies@chara.gsu.edu, huang@chara.gsu.edu, mcswain@chara.gsu.edu*

M. A. Stark<sup>2</sup>

*Department of Astronomy and Astrophysics, The Pennsylvania State University, 525  
Davey Laboratory, University Park, PA 16802*

*stark@astro.psu.edu*

A. van der Meer, and L. Kaper

*Astronomical Institute "Anton Pannekoek", University of Amsterdam, Kruislaan 403,  
NL-1098 SJ Amsterdam, Netherlands*

*ameer@science.uva.nl, lexk@science.uva.nl*

## ABSTRACT

We present spectroscopy of the microquasar SS 433 obtained near primary eclipse and disk precessional phase  $\Psi = 0.0$ , when the accretion disk is expected to be most "face-on". The likelihood of observing the spectrum of the mass donor is maximized at this combination of orbital and precessional phases since the donor is in the foreground and above the extended disk believed to be present in the system. The spectra were obtained over four different runs centered on these special phases. The blue spectra show clear evidence of absorption features consistent with a classification of A3-7 I. The behavior of the observed lines indicates an origin in the mass donor. The observed radial velocity variations are in anti-phase to the disk, the absorption lines strengthen at mid-eclipse when the donor star is expected to contribute its maximum percentage of the total flux, and

---

<sup>1</sup>Visiting Astronomer, Kitt Peak National Observatory, National Optical Astronomical Observatories, which is operated by the Association of Universities for Research in Astronomy, Inc. (AURA) under cooperative agreement with the National Science Foundation.

<sup>2</sup>Guest Observer, McDonald Observatory of the University of Texas at Austin.

the line widths are consistent with lines created in an A supergiant photosphere. We discuss and cast doubt on the possibility that these lines represent a shell spectrum rather than the mass donor itself. We re-evaluate the mass ratio of the system and derive masses of  $10.9 \pm 3.1 M_{\odot}$  and  $2.9 \pm 0.7 M_{\odot}$  for the mass donor and compact object plus disk, respectively. We suggest that the compact object is a low mass black hole.

In addition, we review the behavior of the observed emission lines from both the disk/wind and high velocity jets.

*Subject headings:* stars: individual (SS 433, V1343 Aquilae) — X-rays: binaries — star: winds, outflows — stars: individual (HD 9233) — supergiants

## 1. INTRODUCTION

The well-studied binary SS 433, despite the wealth of observational and theoretical studies, is still one of the most enigmatic systems. SS 433 is an X-ray binary consisting of a compact star and a mass donor star, called such because it donates mass to a precessing extended disk surrounding the compact companion, typically considered to be a black hole (e.g. Leibowitz 1984) or neutron star (e.g. D’Odorico et al. 1991). SS 433 is also well known as a source of collimated relativistic jets with speeds  $v_{jet} \approx 0.26c$  (e.g. Margon 1982). The number of components in this system combined with their complexity greatly obscures interpretation of observational data and theoretical modeling, and thus many physical parameters of the system are as yet undetermined.

The 13 day orbital period of the binary as well as the 162 day period of the disk precession are well established (Goranskii et al. 1998; Eikenberry et al. 2001; Gies et al. 2002). The radial velocity behavior of the compact companion and inner disk, while complicated by emission from other components, has also been convincingly established with a semiamplitude of  $\approx 170 \text{ km s}^{-1}$  (Fabrika & Bychkova 1990; Gies et al. 2002). Antokhina & Cherepashchuk (1987) suggested that observation of the mass donor spectrum could be possible and would lead to direct kinematical masses for the two components. An accurate detection of the mass donor spectrum is crucial in determining if the compact companion is a black hole or neutron star. A first attempt at this was made by Gies, Huang, & McSwain (2003, = GHM03) who found similarities between absorption features in the mid-eclipse spectrum of SS 433 and an A-type evolved star, specifically the A7 Ib star HD 148743. Their detection provided a tentative determination of the radial velocity curve of the mass donor resulting in a mass determination for both components. We set out to confirm this tentative detection of the mass donor with additional observations.

Absorption features from the mass donor star may best be observed during primary eclipse (donor star inferior conjunction) when much of the continuum light from the disk is blocked and the donor star is in the foreground. The precession of the extended disk complicates detection of the mass donor since we expect the disk to have both a high opacity and large vertical extent. This means that light from the mass donor will be obscured by the disk except near precessional phase zero, the phase of maximum disk opening. The combination of precessional phase  $\Psi = 0.0$  and orbital phase  $\phi = 0.0$  limits the possible observing times to roughly two five-night windows per year.

Here we present new spectroscopy of SS 433 at three epochs corresponding to  $\Psi = 0.0$  and  $\phi = 0.0$  that we combine with the original data from GHM03. We show that the absorption spectrum is well matched by the spectrum of HD 9233, an A4 Iab star. We also utilize the emission features in the spectrum to confirm both the orbital and precessional phases of observation. The observed jet features and the “stationary” emission lines are also discussed.

## 2. Observations and Reductions

The spectra of SS 433 were obtained during four epochs of observation. We obtained spectra during 2002 June, 2002 November, and 2003 April with the Large Cassegrain Spectrograph on the 2.7m Harlan J. Smith Telescope at the University of Texas McDonald Observatory. The fourth epoch spectra were obtained with the RC Spectrograph at the Mayall 4m telescope at Kitt Peak National Observatory in 2003 October. Two different CCDs, the TI1 and CC1 arrays, were used during the McDonald Observatory runs. During the 2002 November run we used the CC1 array, which unfortunately produced a low S/N ratio. The first night of the 2003 April run also used this CCD, but the remaining nights utilized the TI1 array in a successful attempt to improve the results. Table 1 provides a list of the mid-exposure heliocentric Julian date, observatory of origin, wavelength coverage, reciprocal dispersion, resolving power, and S/N ratio in the continuum (near 4600 Å) for each night of the four observing runs. The KPNO observations include wavelengths out to 4940 Å, though internal vignetting limits quantitative analysis to wavelengths blueward of about 4800 Å. The final two columns provide the calculated precessional ( $\Psi$ ) and orbital ( $\phi$ ) phases of each observation. For orbital phase we use the light curve ephemeris of Goranskii et al. (1998),

$$\text{HJD } 2,450,023.62 + 13.08211E$$

and for disk precession the model ephemeris of Gies et al. (2002),

$$\text{HJD } 2,451,458.12 + 162.15E.$$

The spectra were reduced using standard routines in IRAF<sup>1</sup>. All the spectra from an individual night were coadded to improve the S/N ratio. No phase shifts were introduced during coaddition since the total observing time each night ( $< 4$  hrs) is negligible relative to the orbital period. The coadded spectra were then shifted to a heliocentric frame and rectified to a unit continuum by fitting regions free from emission lines. The continuum rectification arbitrarily removes the continuum variations caused by the eclipse occurring during the observation intervals. All of the spectral intensities in this paper are set relative to the continuum, which changes on a night-to-night basis.

### 3. The Emission Spectrum of SS 433

We begin by considering the emission lines that dominate the appearance of the blue spectrum of SS 433 and that can be used to verify the orbital and precessional phases of our observations. Figure 1 shows the spectra obtained nearest to mid-eclipse from each of the four runs. The emission features can generally be grouped into two categories, the “stationary” lines, which presumably originate in or near the disk (Crampton, Cowley, & Hutchings 1980; Crampton & Hutchings 1981), and the relativistic jet lines. Both sets of lines typically show variability from night-to-night and run-to-run in strength, structure, and velocity. Here we discuss the variations in strength and velocity of the emission features in our spectra for both sets of lines.

#### 3.1. Collimated Jet Lines

Figure 2 shows the progression of the blue-shifted  $H\beta$  jet line ( $H\beta-$ ) during the 2002 June and 2003 March runs at McDonald Observatory and the apparent absence of jet lines during the 2003 October run at KPNO. Upon closer inspection, we do find a weak jet line blended with the  $H\gamma$  line on night one of the KPNO run. We isolated the jet line for measurement by scaling the night two spectrum by the peak  $H\gamma$  intensities and subtracting it from the night one spectrum. It is interesting that the remaining nights do not show evidence of optical jet lines. Instances in which the jet lines disappear for days at a time have been noted in the past and while not common, are not exceedingly unusual (Margon et al. 1984; Gies et al. 2002).

---

<sup>1</sup>IRAF is distributed by the National Optical Astronomical Observatories, which is operated by the Association of Universities for Research in Astronomy, Inc., under cooperative agreement with the National Science Foundation.

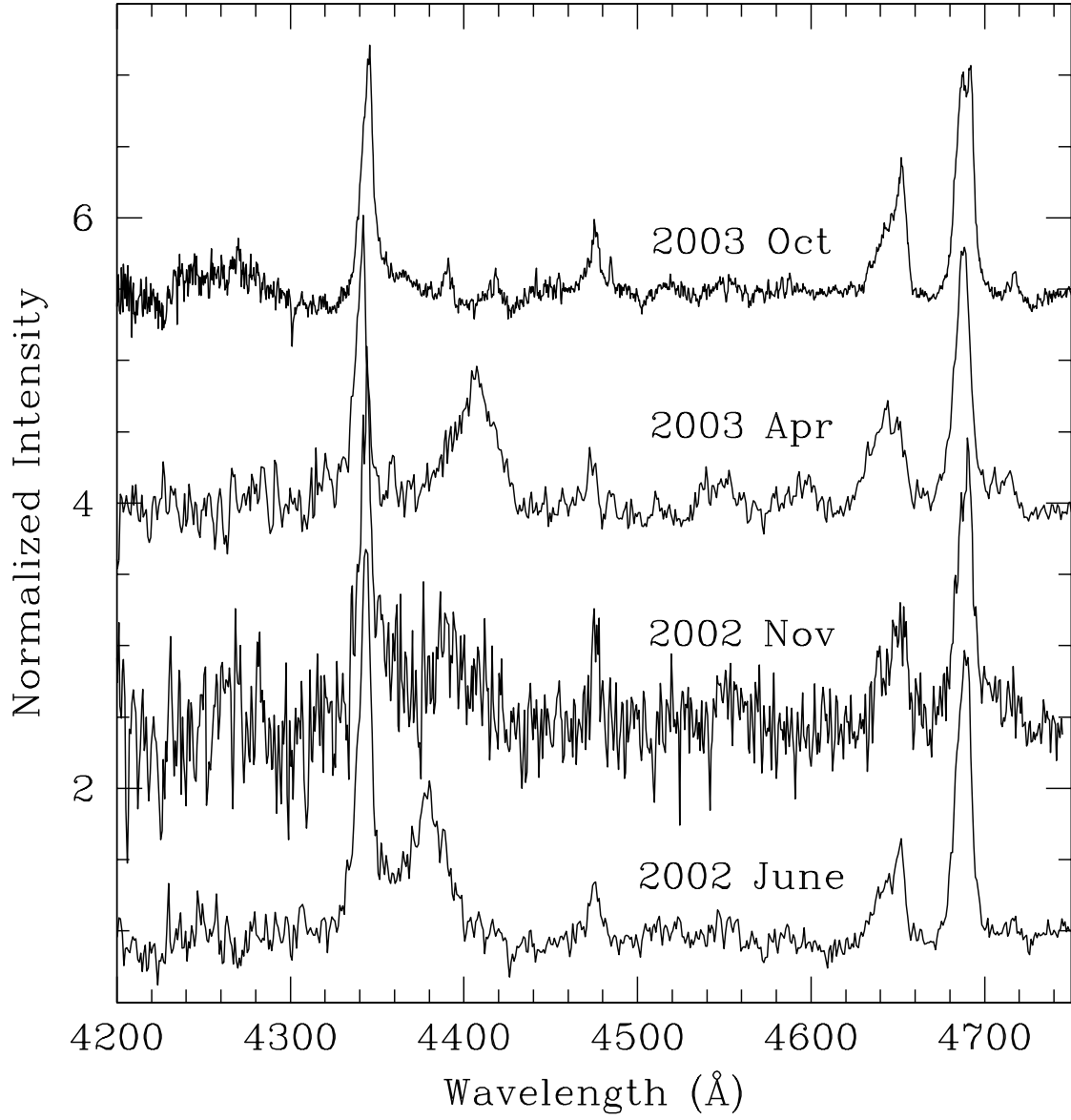


Fig. 1.— SS 433 spectra obtained closest to mid-eclipse for each of the four observing runs. The continua are set at 1.0, 2.5, 4.0, and 5.5 in normalized intensity units for clarity of separation.

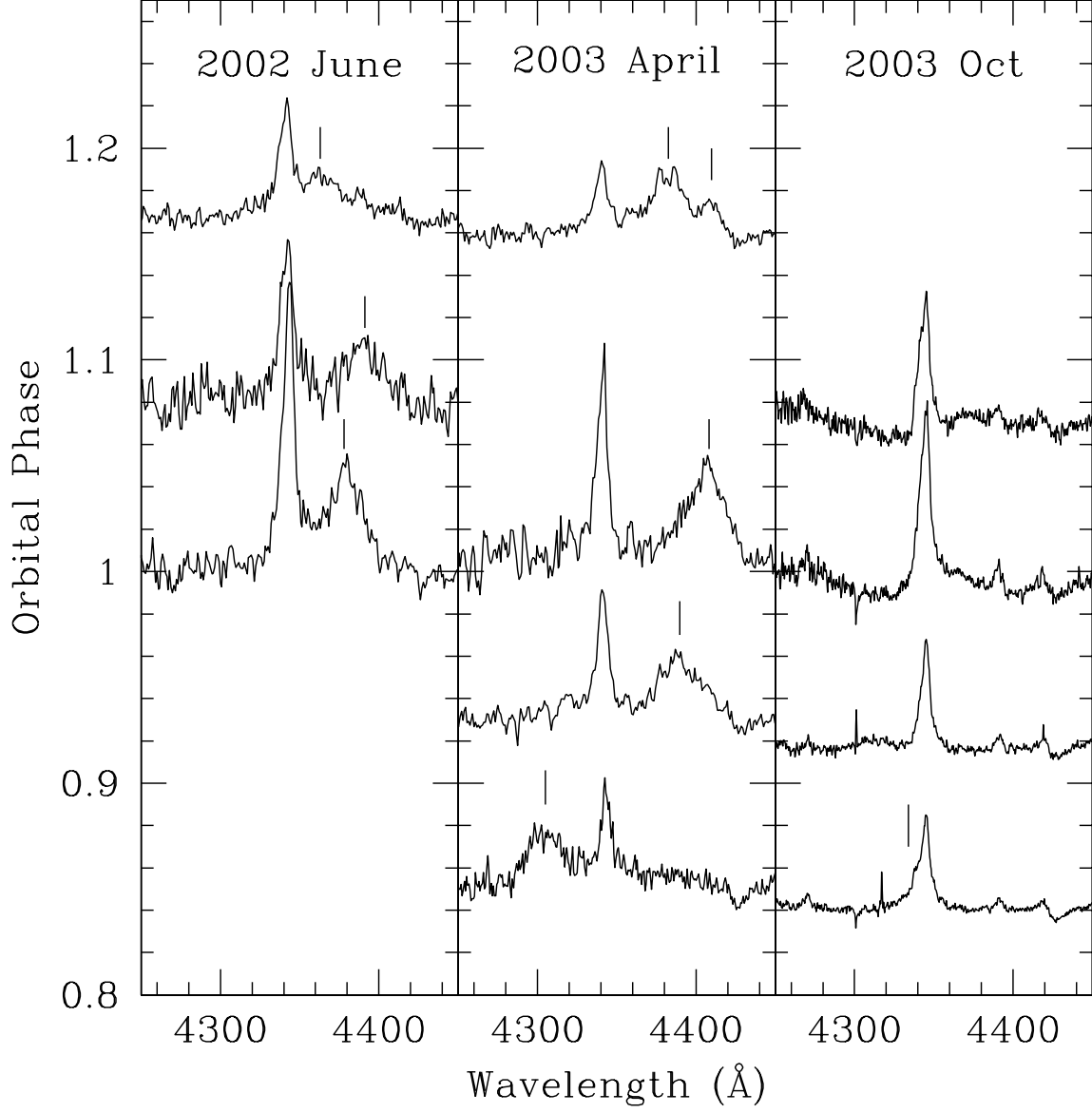


Fig. 2.— The variability in velocity and strength of H $\beta$ – jet lines for the three epochs with more than one observation. The spectra are scaled so that their continuum corresponds to the orbital phase of observation. Jet line positions are indicated by vertical tick marks. H $\gamma$  emission is detected at 4340 Å.

Velocity changes in the jet lines from one night to the next are due primarily to the “nodding” motion of the disk caused by the orbiting mass donor (Katz et al. 1982; Gies et al. 2002). Gies et al. (2002) produced a model fit of the disk nodding for related jet motions of the  $H\alpha+$  and  $H\alpha-$  jet lines. They treat the lines as individual “bullets” best measured via Gaussian fits of distinct peaks. We use this method (see Table 2) and their model fit to illustrate the Doppler shifts in Figure 3. The solid line in the figure is the radial velocity curve from Gies et al. (2002) for the  $H\alpha-$  jet feature. Each dot represents an observed jet feature and the area of the dot is proportional to the measured equivalent width of the feature. In the last three nights of the 2003 April spectra, the jet lines are blended with the diffuse interstellar band at 4430 Å. To remove its effect, the normalized spectrum from night one was set to an average value of zero (by subtracting 1.0 from each point) and then subtracted from the remaining three nights. The equivalent widths were then measured for these nights from the subtracted spectra.

Two independent “bullets” were measured in the last spectrum from 2003 April, giving two plotted points in Figure 3. One of these is at the same velocity as the feature measured in the previous spectrum and is likely the remnant of that feature. The tentative jet feature that we identified in the first spectrum from the KPNO run is included in Figure 3 and the good match between its velocity and the model velocity curve suggests that this is indeed a jet emission line. It is clear from Figure 3 that the parameters found by Gies et al. (2002) are still appropriate when applied to data for the  $H\beta-$  jet obtained up to five years later. Figure 3 also establishes that our spectra were indeed taken around precessional phase  $\Psi = 0.0$  (minimum  $z$  for the  $H\beta-$  jet).

### 3.2. Stationary Emission Lines

Because our spectra are not flux calibrated we need a different method to confirm that we were indeed observing the system during primary eclipse. Gies et al. (2002) and GHM03 point out that many of the emission lines are expected to form in a volume larger than that of the inner disk. Lines of this type would show a small decrease in absolute flux during eclipse. On the other hand, emission lines formed in the inner regions of the disk should also be eclipsed by the donor star and should show a corresponding drop in absolute flux.

With our rectified continuum, the *apparent* behavior of these lines would be different. As the continuum light decreases, the “wind” lines would appear to increase in strength (relative to the continuum) while the inner disk lines should remain roughly constant in strength (again, relative to the continuum). The  $H\gamma$ , He I  $\lambda 4471$ , and possibly He II  $\lambda 4686$  emission lines are expected to be “wind” lines. By measuring the strength of these lines

Table 1. Information for the four epochs of observation

Date (HJD - 2,450,000)	Observatory	$\lambda$ range (Å)	Dispersion (Å pixel <sup>-1</sup> )	$R$ ( $\lambda/\Delta\lambda$ )	S/N ratio (res. element <sup>-1</sup> )	$\Psi$	$\phi$
2430.762.....	McDonald	4060–4750	0.889	2600	31	0.998	0.003
2431.823.....	McDonald	4060–4750	0.889	2600	16	0.004	0.084
2432.938.....	McDonald	4060–4750	0.889	2600	40	0.012	0.169
2590.037.....	McDonald	4035–4745	0.694	3300	9	0.965	0.988
2755.873.....	McDonald	4070–4790	0.703	3300	42	0.003	0.854
2756.873.....	McDonald	4060–4760	0.887	2600	66	0.010	0.931
2757.870.....	McDonald	4060–4760	0.887	2600	24	0.016	0.007
2759.878.....	McDonald	4060–4760	0.887	2600	60	0.028	0.160
2912.695.....	KPNO	4180–4940	0.372	6200	183	0.971	0.842
2913.692.....	KPNO	4180–4940	0.372	6200	102	0.977	0.918
2914.697.....	KPNO	4180–4940	0.372	6200	81	0.983	0.995
2915.689.....	KPNO	4180–4940	0.372	6200	66	0.989	0.071

Table 2. Emission line equivalent widths and jet-line radial velocities

Date (HJD-2,450,000)	$z$ (Jet)	$W_\lambda$ (Å)				
		Jet	H $\gamma$	He I $\lambda$ 4471	N III/C III	He II $\lambda$ 4686
2430.762 .....	−0.099	−18.1	−16.8	−3.3	−10.2	−22.4
2431.823 .....	−0.097	−16.5	−13.1	−1.0	− 7.6	−17.1
2432.938 .....	−0.103	−14.4	− 6.5	−0.7	− 7.7	−11.4
2590.037 .....	−0.096	−14.7	−14.7	−2.8	− 9.0	−16.2
2755.873 .....	−0.115	−10.5	− 4.3	−0.4	− 5.5	− 6.7
2756.873 .....	−0.097	−17.8	− 7.4	−1.0	− 8.1	−12.0
2757.870 .....	−0.093	−21.5	−12.2	−2.3	−11.6	−16.4
2759.878 .....	−0.093	− 5.0	− 4.5	−1.1	− 5.6	− 8.6
2759.878 .....	−0.098	−10.8	...	...	...	...
2912.695 .....	−0.109	− 2.6	− 6.3	−0.7	− 8.6	−10.4
2913.692 .....	...	...	− 8.4	−0.9	− 8.4	−12.5
2914.697 .....	...	...	−13.6	−2.5	−11.7	−20.2
2915.689 .....	...	...	−12.0	−1.8	−10.7	−15.8



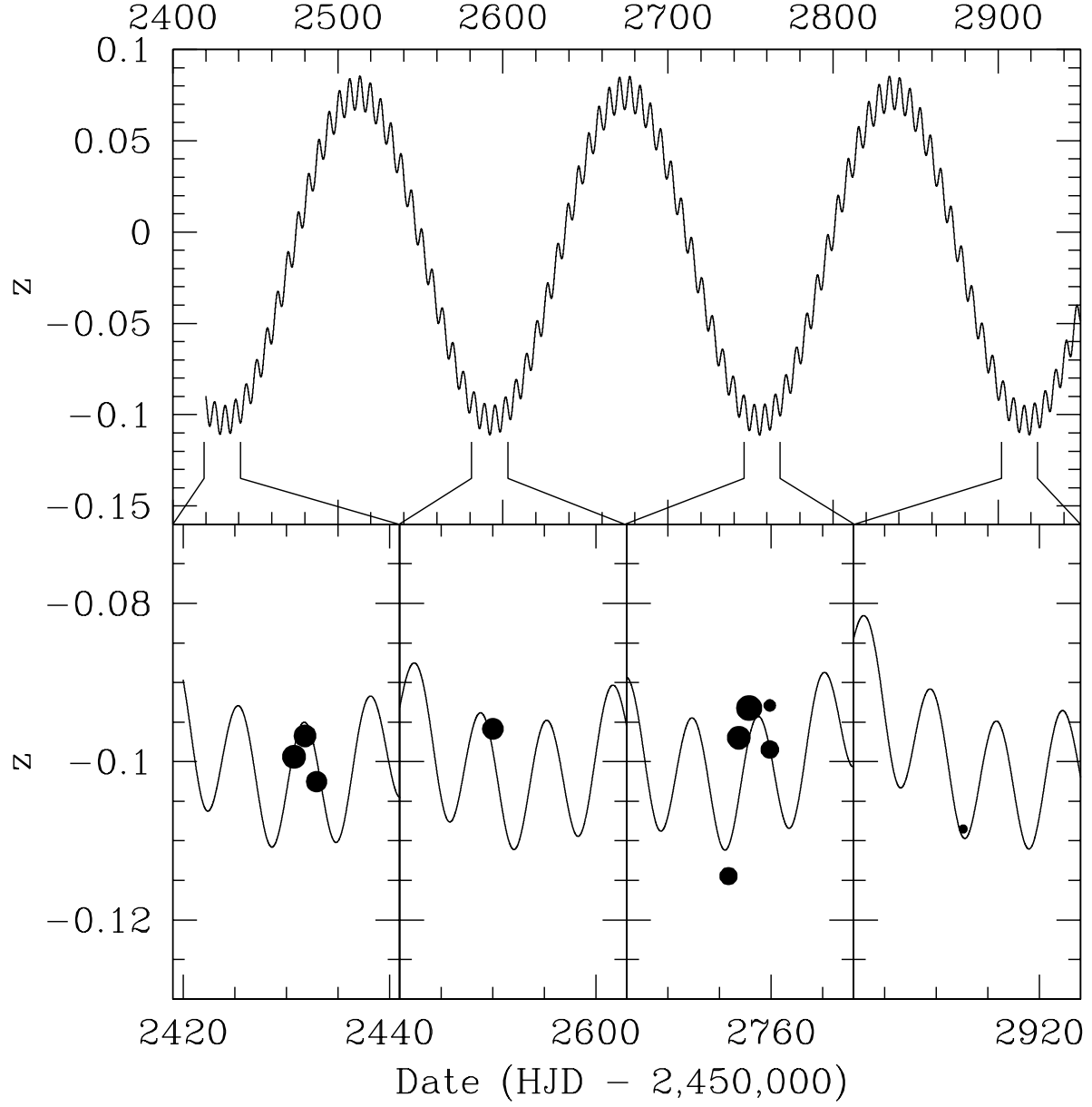


Fig. 3.— The model of expected approaching jet line velocity from Gies et al. (2002) along with our measured jet features. Point area is plotted proportional to equivalent width.

relative to the continuum, we can test that our observations did indeed take place during eclipse. The origin of the N III/C III complex at  $\lambda 4650$  is less certain, though for completeness we measure it as well.

Our measured values for the equivalent width of the major emission lines are given in Table 2. The average errors for measurements in the table are  $\sigma_z \approx 0.001$  and  $\sigma_{W_\lambda} \approx 0.1 \text{ \AA}$ . Figure 4 shows the relative strengths of each of the four emission features for each run. We also show a schematic representation of the expected variations through eclipse of a constant flux source in our continuum-rectified versions of the spectra. The  $B$ -band flux variation was estimated by a spline fit through the average magnitude in each 0.05 phase bin of the  $V$ -band light curve for  $\Psi = 0.0$  from Goranskii et al. (1998, see their Fig. 7(c)) adjusted for the  $B - V$  color variation reported by Goranskii et al. (1997, see their Fig. 3). The strengths of the measured emission features are normalized in each case to best match the schematic eclipse curve. The  $H\gamma$ , He I  $\lambda 4471$ , and He II  $\lambda 4686$  lines all show a clear eclipse effect centered on the night in each run with calculated orbital phase closest to  $\phi = 0.0$  and they all appear to match the general behavior of the eclipse light curve. This confirms that our ephemeris was correct and that our spectra were taken during primary eclipse.

We also see from Figure 4 that the N III/C III complex does not show such clear variations. The 2003 April McDonald data (*open squares*) show behavior very much like that seen in the other wind lines. During the remaining runs, however, this feature shows only a small modulation near  $\phi = 0.0$ . It is likely that the N III/C III lines are confined to more interior regions of the disk and that during the 2003 April run the N III/C III emitting region had expanded.

#### 4. The Absorption Spectrum of SS 433

In order to best identify the absorption spectrum of the mass donor star, we identified a portion of the continuum that was free of large emission lines. The best available region in our spectra extends from 4510–4625 $\text{\AA}$  (Fig. 1). This range avoids the interstellar absorption at 4502 $\text{\AA}$ , emission from He I  $\lambda 4471$ , and the N III/C III emission complex which begins near 4630 $\text{\AA}$ . Since the 2003 October KPNO spectra have the highest S/N ratio and resolution, we compared the mid-eclipse spectrum by eye with spectra of the comparison stars that we observed. Because GHM03 had not found a good match with the spectra of an O or B-type star, but had identified possible matches with an A-type supergiant, we obtained spectra during the KPNO run of supergiants of types A4 Iab, F5 I, and G8 Iab. During the previous McDonald runs we obtained spectra of stars of type B1 Iab, B5 Ib, A0 Ib, A7 Ib, and F0 Iab.

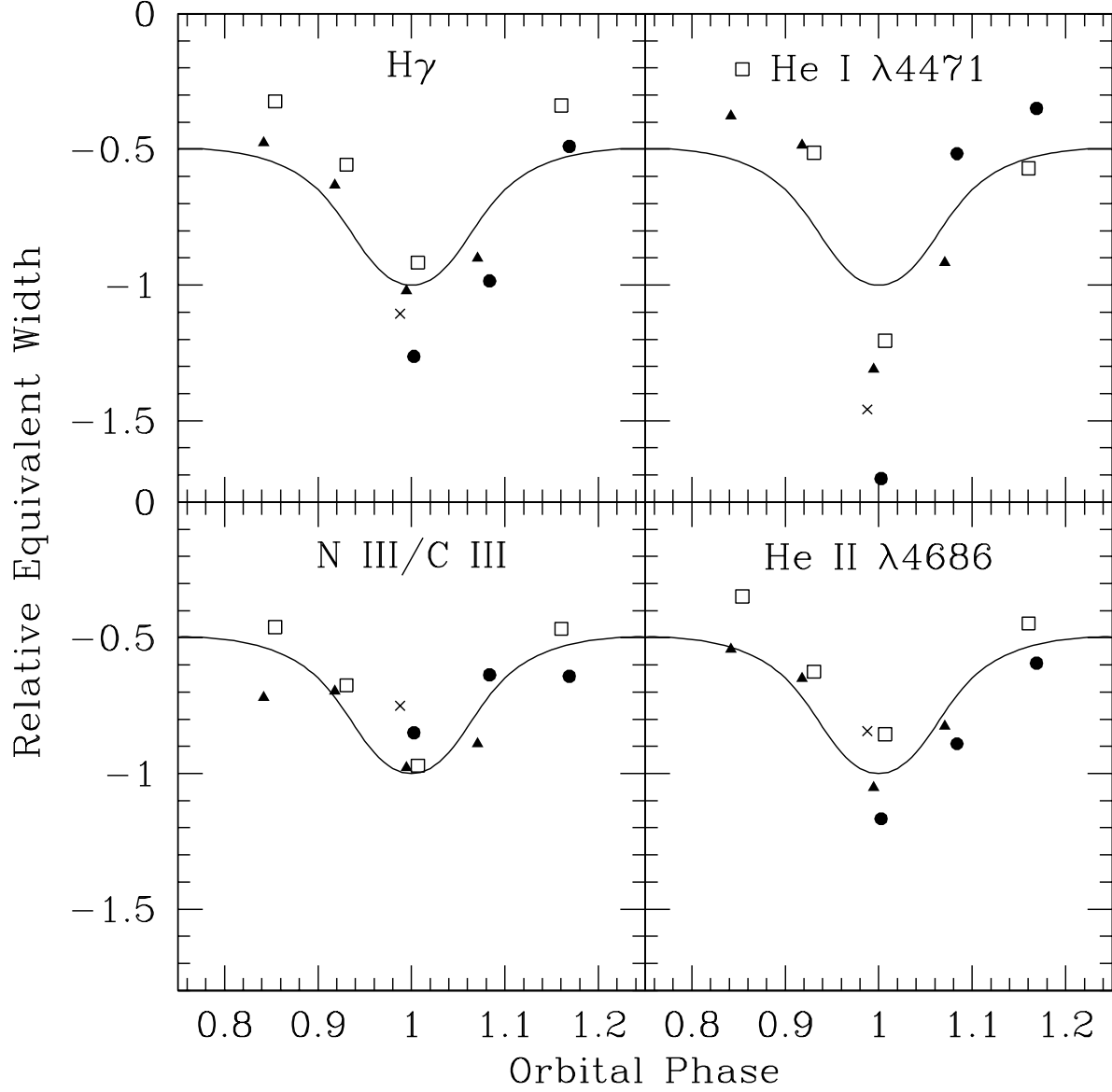


Fig. 4.— Equivalent width measurements for the four major emission features seen in spectra from all four observing runs plotted vs. orbital phase. Filled circles represent the 2002 June McDonald run, x's the 2002 November McDonald observation, open squares the 2003 April McDonald run, and filled triangles the 2003 October KPNO run. The solid line is a schematic representation of the expected variations based upon the  $B$ -band eclipse light curve, derived from Goranskii et al. (1997, 1998)

The A4 Iab spectrum (of HD 9233) appeared to have a significant number of features in common with the absorption line patterns in the chosen continuum region of SS 433. The spectra were boxcar smoothed by 3 pixels to increase the S/N ratio and again compared by eye. The apparent correlation between the two spectra became more obvious. The smoothed spectra of SS 433 (*solid line*) and HD 9233, the A4 Iab star (*dashed line*), are shown overplotted in Figure 5. The A4 Iab spectrum has been Doppler-shifted according to the relative velocity shift found via cross-correlation functions (CCFs), as described below. We have also applied an intensity scaling factor to the A star spectrum to match the equivalent widths of the absorption features in SS 433. Because of the continuum light contribution of the disk/wind, the spectrum of the mass donor will be veiled. The depth of the absorption features will be smaller relative to the continuum than in the case of HD 9233 where the A star is the only continuum source. The applied correction factor is  $0.36 \pm 0.07$ , so that the lines in the A star spectrum are plotted with 36% of their observed strength. If the absorption spectrum belongs to the donor star then this comparison tells us that the mass donor in SS 433 contributes  $\approx 36\%$  of the total light at mid-eclipse.

The spectrum of SS 433 in Figure 5 has been highly rectified to remove any low-order variations in the spectra (compare Fig. 5 with Fig. 1) since we are attempting to match only high-order variations—the narrow absorption lines. We have labeled a number of the strongest absorption lines with their element, species, wavelength, and multiplet number. It is interesting to note that the lines which seem to match least well correspond to the Fe II (37) multiplet, yet the Fe II (38) multiplet lines are all well matched. In addition to that of the A4 Iab star, the spectrum of the A7 Ib supergiant HD 148743 also appeared to fit the spectrum of SS 433 quite well. The lower resolution of the McDonald spectrum of HD 148743, however, did not provide as useful a comparison to the higher S/N ratio spectra from the 2003 October KPNO run. None of the remaining spectral standard stars that we observed provided as good a match with the SS 433 spectrum.

In order to quantify the correlation between the SS 433 spectrum and the A4 Iab spectrum, we cross-correlated all of the SS 433 spectra with the intensity scaled spectrum of HD 9233. The A4 Iab spectrum was smoothed to the resolution of the spectra for each of the McDonald runs using a Gaussian smoothing algorithm.

All four of the 2003 October KPNO spectra produced CCFs which showed a strong correlation peak. The single McDonald spectrum from the 2002 November run was simply too noisy for a good cross-correlation. The spectra from the two remaining McDonald runs of 2002 June and 2003 April did not provide conclusive correlations due to low S/N ratios. Peaks were present in the CCFs for these runs near the expected velocity shifts, but they were not clearly significant when compared to the “noise” in the CCF. By overplotting the

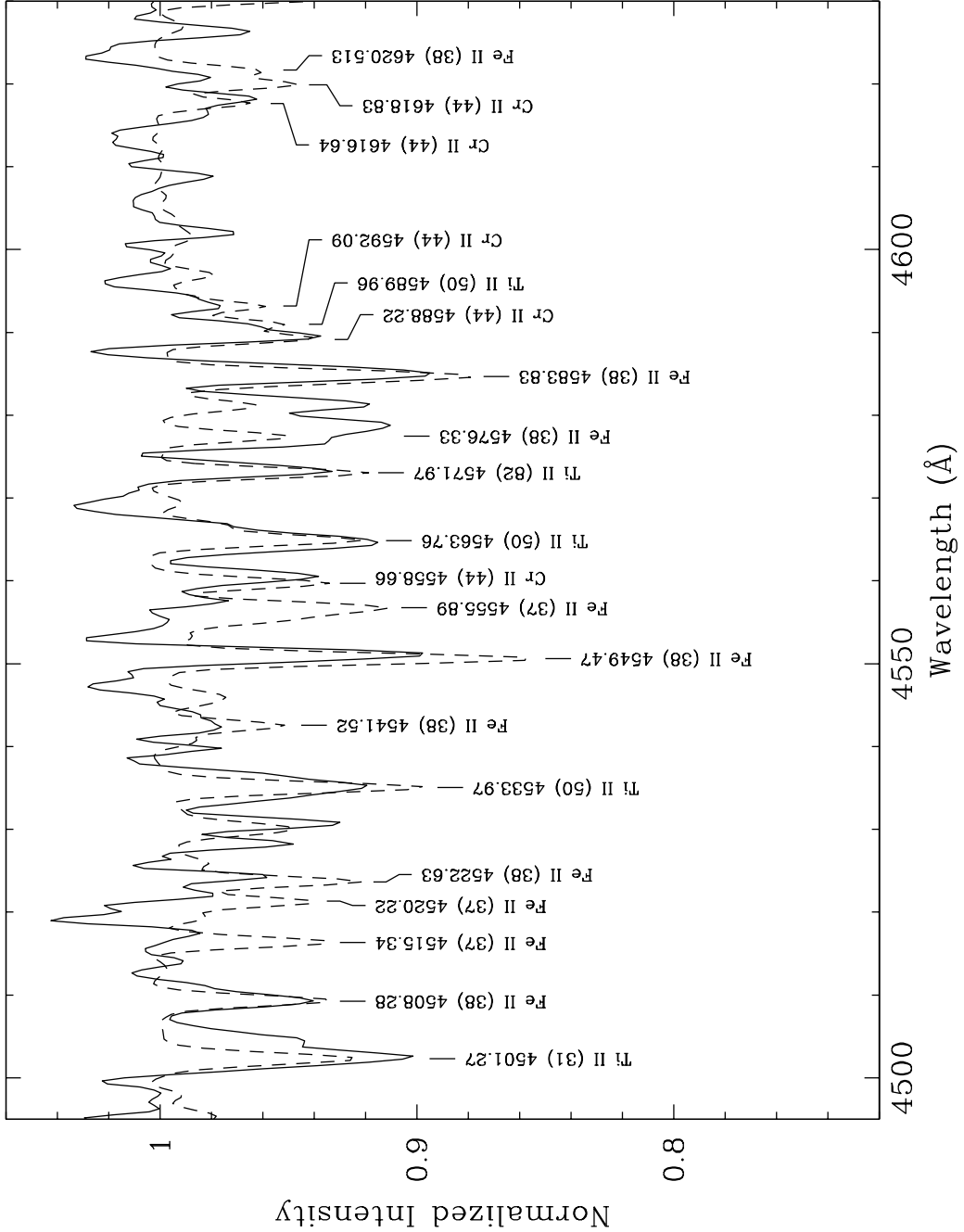


Fig. 5.— An overplot of the continuum region of SS 433 from night three (near mid-eclipse) of the 2003 October KPNO run (*solid line*) and the A4 lab star HD 9233 (*dashed line*). The spectrum of HD 9233 has been Doppler-shifted and intensity scaled by 36% to match the spectrum of SS 433 (see text).

A4 spectrum, we found that a number of major absorption lines did appear in common. While this alignment of features was significant enough in the 2002 June spectra for GHM03 to produce a tentative classification, as mentioned previously, the S/N ratio was simply not high enough to produce a clear correlation.

A comparison of the strengths of the Ti II, Cr II, and Fe II absorption lines in both spectra shows that the relative depths of absorption features in SS 433 are very similar to that in HD 9233. The S/N ratio severely limits this analysis, but we can say that the overall pattern of lines visible in SS 433 appears much more like the A4 spectrum than the F0 or A0 McDonald spectra. Therefore, considering the cross-correlation results and visual inspection, we tentatively classify the absorption spectrum as A3-7 I, with a corresponding effective temperature of  $T_{\text{eff}} = 8500 \pm 1000$  K (Venn 1995).

We expect that absorption lines from the mass donor should increase in strength relative to the continuum as SS 433 goes into eclipse and a larger fraction of the observed light is coming from the donor star. This should be followed by a decrease in relative strength during egress of the eclipse. This trend should appear in the CCFs as an increase, then decrease in the amplitude of the peak. The relative CCF peak amplitudes for the KPNO spectra are measured to be 0.34, 0.64, 1.00, and 0.69 from first to fourth night, respectively. The approximate error on the amplitudes is  $\pm 0.08$ . We would expect that the strength of absorption features from the mass donor and emission lines originating in the extended disk wind should behave similarly during eclipse. Figure 6 shows the absorption line cross-correlation amplitude variation plotted similarly to the emission line equivalent widths in Figure 4. Also shown is the prediction of the variation for a constant flux source based upon the estimated *B*-band light curve (*solid line*). The differences in the observed and predicted variation are qualitatively what would be expected if the donor star is being obscured as it descends into an extended disk.

The CCFs also provide us with measurements of the radial velocities of the absorption features relative to those of HD 9233. To convert these to absolute radial velocities, we used Gaussian fits to measure velocities for 13 lines in the spectrum of HD 9233. The average of these lines produced a radial velocity measure for HD 9233 of  $-34 \pm 2$  km s<sup>-1</sup>, which we added to the relative velocities of the CCFs. Our values for  $V_r$  are given in Table 3 for the four 2003 October KPNO spectra.

Although constructing a radial velocity curve from only four points is difficult, most of the orbital parameters for SS 433 are already known. With the light curve ephemeris of Goranskii et al. (1998), as used above, the only remaining parameters for the radial velocity curve of the mass donor are systemic velocity,  $\gamma$ , and semi-amplitude,  $K_O$ . We use subscripts

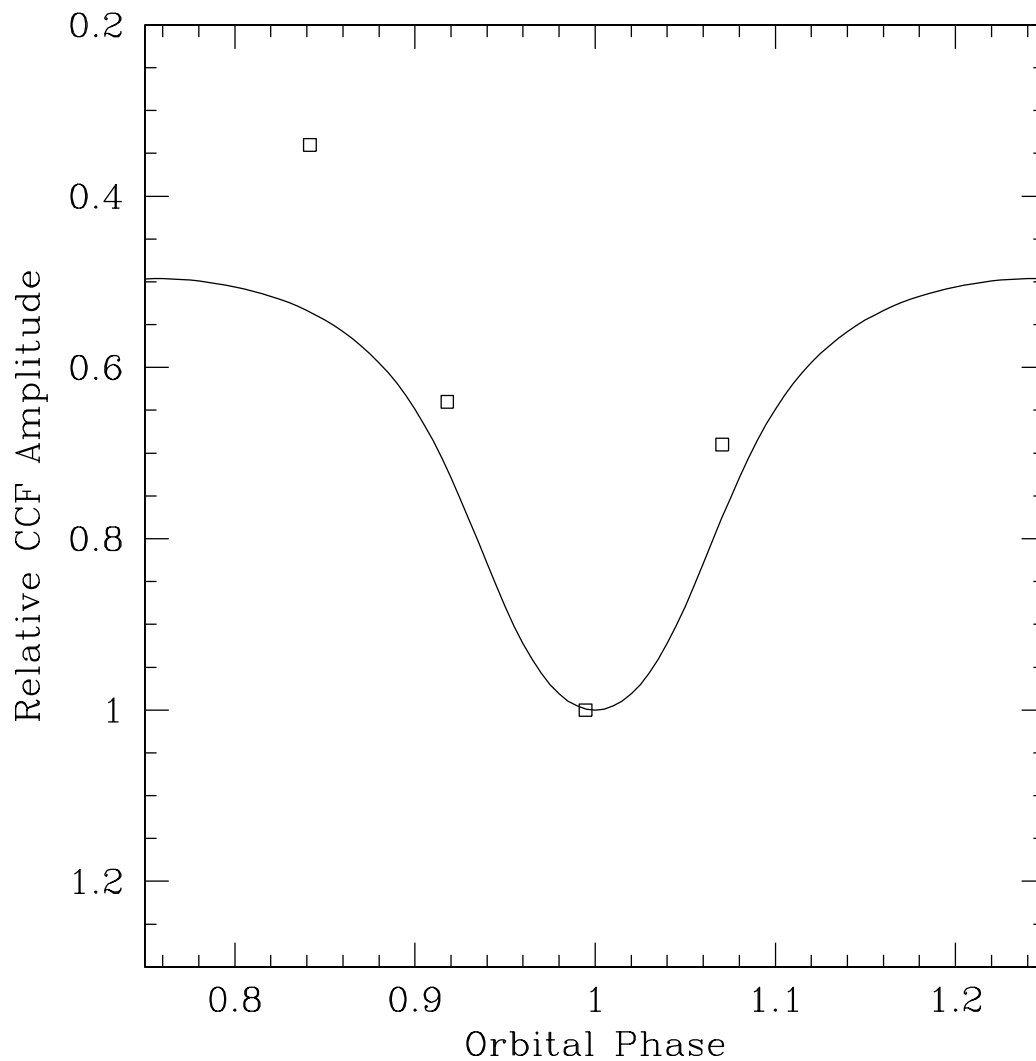


Fig. 6.— Cross-correlation amplitudes for the absorption features of the four spectra from the 2003 October KPNO run (*squares*). Also shown is the predicted variation for a constant flux source (*solid line*) based upon the schematic *B*-band light curve (see text).

$O$  and  $X$  to distinguish the motion of the optical star and the compact X-ray source. Using a non-linear least squares routine, we fit our four radial velocities with a sine curve, assuming zero orbital eccentricity (Fabrika & Bychkova 1990). The resulting fit gives  $\gamma = 65 \pm 3$  km s<sup>-1</sup> and  $K_O = 45 \pm 6$  km s<sup>-1</sup>. Figure 7 shows our four radial velocity points and the best-fit sine curve.

Fabrika & Bychkova (1990) give a semi-amplitude for the compact object and disk of  $K_X = 175 \pm 20$  km s<sup>-1</sup> and Gies et al. (2002) give  $K_X = 162 \pm 29$  km s<sup>-1</sup>. Taking the average of these two,  $K_X = 168 \pm 18$  km s<sup>-1</sup>, we arrive at a mass ratio,  $q = M_X/M_O = K_O/K_X = 0.27 \pm 0.05$ . This value of  $q$  is interestingly near the convergence of the two mass ratio predictions of Antokhina & Cherepashchuk (1987) and Antokhina et al. (1992). From optical light curve modeling, Antokhina & Cherepashchuk (1987) arrive at a mass ratio lower limit,  $q \geq 0.25$ . However, from X-ray eclipse models, Antokhina et al. (1992) arrive at a range of possible mass ratios,  $q = 0.15\text{--}0.25$ . Our value of  $q = 0.27$  is consistent with both suggestions, falling at the intersection of these two models.

In addition to velocities, we can also model the projected rotational velocity  $v_{rot} \sin i$  of the star. The modeling was done by comparing theoretical line broadening functions to our observed spectra. The instrumental broadening, found from our comparison spectra, is 22.5 km s<sup>-1</sup>. A Gaussian with this width ( $\sigma$ ), was broadened assuming a spherical star with a linear limb-darkening coefficient of 0.57 (Wade & Rucinski 1985). A grid of theoretical profiles was computed for a range of  $v_{rot} \sin i$  values and a  $\chi^2$  minimization was used to determine the best fit to the data. For the mid-eclipse spectrum from KPNO, which has the deepest lines, the average  $v_{rot} \sin i$  of the eight strongest lines is  $80 \pm 20$  km s<sup>-1</sup>. The same lines for the A4 lab star HD 9233 give a  $v_{rot} \sin i$  of  $39 \pm 12$  km s<sup>-1</sup> which is at the upper end of the range found for A supergiants by Venn (1995). Using a system inclination for SS 433 of 78°8 (Margon & Anderson 1989) and assuming  $i_{spin} = i_{orbit}$  gives a rotational velocity,  $v_{rot} \approx 82$  km s<sup>-1</sup>. The cause of the disk precession is unknown, but if precession of the rotating donor star is the cause, then the spin and orbital axes may be misaligned.

Table 3. SS 433 absorption line radial velocities

Date (HJD-2,450,000)	$V_r$ (km s <sup>-1</sup> )	error (km s <sup>-1</sup> )
2912.695 . . . . .	25	6
2913.692 . . . . .	40	5
2914.697 . . . . .	68	4
2915.689 . . . . .	76	7



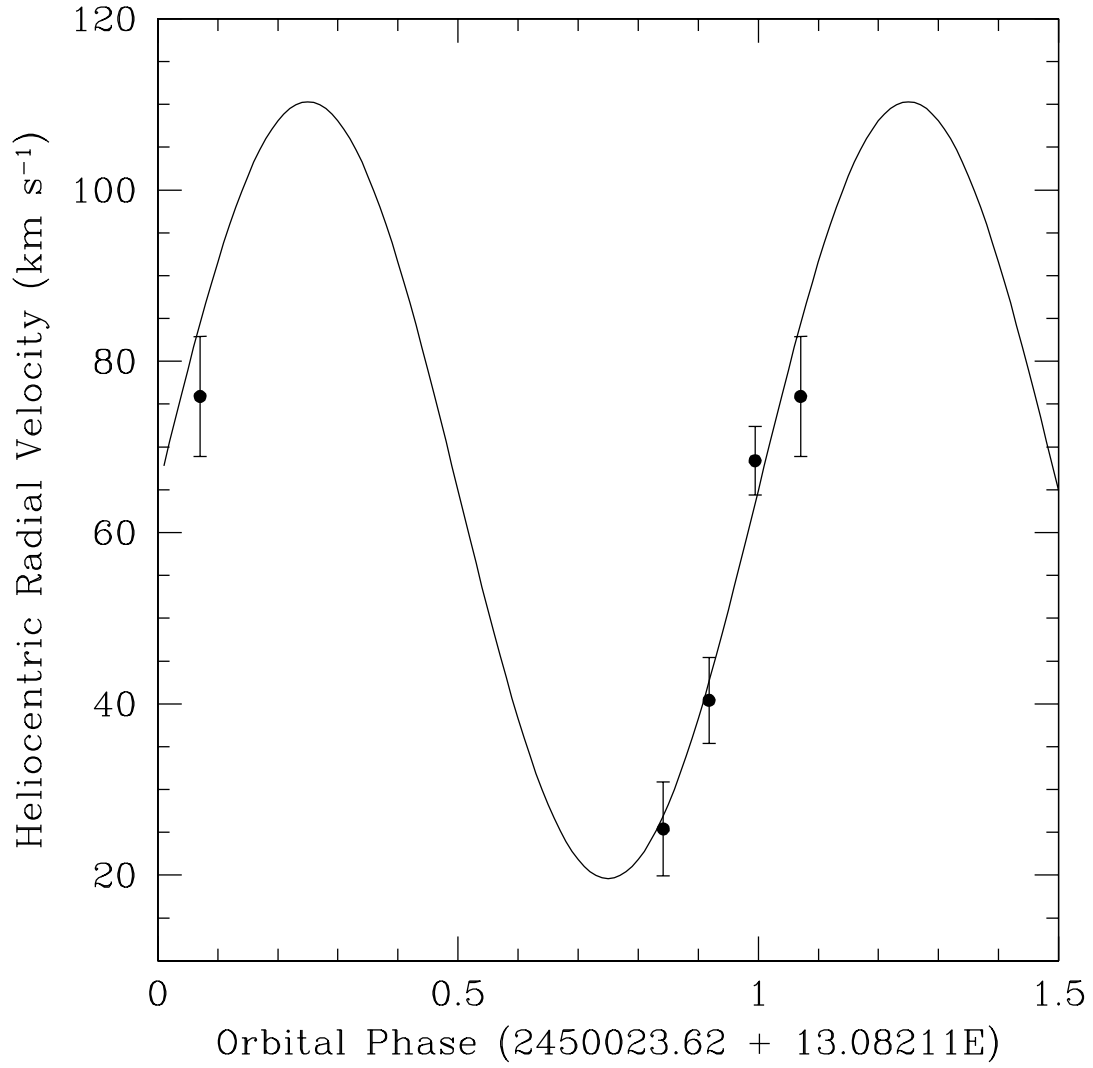


Fig. 7.— The best-fit sine curve to the four radial velocities obtained via cross-correlation fitting of the 2003 October KPNO spectra. All absorption radial velocity values are in a heliocentric rest frame.

## 5. Discussion

From the previous section, we see that the radial velocity curve of the absorption lines is in anti-phase to that of the disk, the resulting mass ratio is within the bounds of existing models of the system, and the magnitude of the CCF amplitude variations with orbital phase is what we might expect if the features originate from the mass donor star. Each of these results points to an origin of the A-type absorption spectrum in the mass donor star. If we assume that these lines do originate in the mass donor, then we can make several further calculations.

We may determine the component masses using the equation

$$M_{O,X} = (1.0361 \times 10^{-7})(\sin i)^{-3}(K_O + K_X)^2 K_{X,O} P M_{\odot},$$

where the semi-amplitudes are in units of  $\text{km s}^{-1}$  and the period is in days. Our value of  $K_O = 45 \pm 6 \text{ km s}^{-1}$  from the above and the average value of  $K_X = 168 \pm 18 \text{ km s}^{-1}$ , along with  $i = 78.8^\circ$  from kinematical models of the jets (Margon & Anderson 1989), result in a mass for the donor star of  $M_O = 10.9 \pm 3.1 M_{\odot}$  and a mass of the compact object/disk of  $M_X = 2.9 \pm 0.7 M_{\odot}$ . Depending on the mass in the disk, our calculated mass may support either a black hole or neutron star as the compact companion. Predictions vary widely regarding the mass of the disk. Collins & Scher (2002) suggest an extremely massive disk, though their system parameters are significantly different from ours. On the other hand, King, Taam, & Begelman (2000) predict a very low mass disk on the basis of evolutionary models. King et al. (2000) also suggest that for a mass donor with  $M_O \gtrsim 5M_{\odot}$  the companion is likely to be a black hole. Observations indicate that all neutron stars have a mass close to  $1.35M_{\odot}$  (Thorsett & Chakrabarty 1999), with the possible exception of Vela X-1 for which a mass near  $1.9M_{\odot}$  has been reported (Barziv et al. 2001; Quaintrell et al. 2003). In light of these results and our calculated mass, and in the absence of a massive disk, we suggest that the compact companion in SS 433 is a black hole rather than a neutron star.

With these masses we can calculate the binary separation and Roche lobe radius for the mass donor. The resulting binary separation from Kepler’s third law is  $a = 0.26 \pm 0.02 \text{ AU} = 56 \pm 4R_{\odot}$ . The volume Roche lobe radius for the mass donor star can be found by (Eggleton 1983)

$$R_L = \frac{0.49q^{-2/3}a}{0.6q^{-2/3} + \ln(1 + q^{-1/3})}$$

which gives  $R_L = 28 \pm 2R_{\odot}$ . This value is approximately the expected radius for an A type supergiant (Venn 1995). The resulting surface gravity is  $\log g = 2.59 \pm 0.14$ .

We can use this value for the Roche lobe radius and the orbital period to derive an expected  $v_{rot}$  for the mass donor if it is synchronously rotating. Assuming synchronous

rotation may not be valid for this system, as described below, but it gives us a quantitative comparison to our measured  $v_{rot} \sin i$ . The resulting value is  $v_{rot} = 108 \pm 7 \text{ km s}^{-1}$ , which is somewhat larger than our estimated value of  $82 \pm 20 \text{ km s}^{-1}$ .

A possible explanation for the difference in observed  $v_{rot}$  and expected synchronous  $v_{rot}$  comes from the SS 433 evolutionary scenario of King et al. (2000). They suggest that SS 433 is undergoing a period of rapid evolution as the mass donor crosses the Hertzsprung gap. This leads to extremely high mass transfer rates. Under these conditions, synchronous rotation is not required and is possibly even unlikely. An alternative explanation is that the spin axis of the mass donor is not aligned with the orbital axis of the system. This type of misalignment may be possible as the result of an asymmetry in the supernova that created the compact companion (Brandt & Podsiadlowski 1995).

The scaling of the HD 9233 spectrum to match the mid-eclipse SS433 spectrum from the 2003 October KPNO run also provides information regarding the origin of the absorption features. The 0.36 scaling factor means that, if these lines do originate in the mass donor, the accretion disk still contributes well over half of the light of the system at mid-eclipse. This is consistent with the findings of Goranskii et al. (1998). They find a 0.41 mag precessional variation in the central eclipse light curve. We must point out though, that our scaling factor was found assuming a mass donor of luminosity type I and our spectrum does not provide sufficient luminosity diagnostics to confirm a luminosity type unambiguously. If the mass donor is of luminosity type II or higher, then the 36% scaling factor would be too low because the metal lines are weaker in higher gravity stars. However, the large mass transfer rate in the system probably indicates that the mass donor fills its Roche lobe, and the mass donor Roche lobe radius found above is consistent with a luminosity type I (Venn 1995).

We can compare our estimated scaling factor with that expected from observed light curves of SS 433. If we assume that the donor star is totally eclipsed by the disk at  $\phi = 0.5$ , then we can use the light curve of Goranskii et al. (1998) to estimate the flux ratio as

$$\frac{F_{\star}}{F(\phi = 0.00)} = \frac{F(\phi = 0.25) - F(\phi = 0.50)}{F(\phi = 0.00)} = 0.29 \pm 0.08.$$

This estimate comes from a comparison of the  $V$ -band light curves of Goranskii et al. (1998) and Kemp et al. (1986). The result matches within errors with our measured scaling factor of  $0.36 \pm 0.07$ . Note that Goranskii et al. (1997) find that the system is slightly redder during mid-eclipse, which implies that the mid-eclipse flux is relatively lower in the  $B$  band compared to the  $V$  band. Thus, the predicted flux contribution of the mass donor in the  $B$  band may be slightly larger than given above. The donor star flux contribution may also be larger if the donor star is not completely eclipsed at  $\phi = 0.50$ .

Regardless of the source of the absorption lines, as long as it is within the system,

we have the systemic radial velocity from fitting the absorption line radial velocity curve. Several distance determinations to SS 433 have arrived at values from 3.0 to 4.85 kpc (e.g. Vermeulen et al. 1993; Dubner et al. 1998; Stirling et al. 2002). Differential galactic rotation curves give the expected system velocity for these distances as 32 and 59 km s<sup>-1</sup>, respectively, for an object stationary with respect to its local standard of rest (Berger & Gies 2001). Our value,  $\gamma = 65 \pm 3$  km s<sup>-1</sup> falls very near the upper end of this range. One must be careful in comparing these two values too closely however since the past supernova in SS433 which resulted in the compact companion may have given the system a runaway velocity (Brandt & Podsiadlowski 1995). The final  $\gamma$  value may therefore not be directly comparable to the results from the differential galactic rotation curve.

The discovery of a mid-A type supergiant spectrum in SS 433 does not necessarily require that the mass donor itself is a mid-A supergiant. One alternative is that we are seeing a “shell” spectrum. The Be star Pleione, for example, shows a narrow line spectrum on top of the broad B star stellar spectrum due to the projection of circumstellar disk gas against the visible hemisphere of the star (Ballereau 1980). This “shell” spectrum closely resembles that of an early A supergiant. Is it possible then that what we are seeing is some form of shell spectrum from SS 433? We doubt this origin for several reasons. First, since our CCFs show a variation in amplitude, with the lines appearing stronger nearest mid-eclipse, the shell spectrum must be physically associated with the mass donor. In other words, the absorption taking place is absorption of continuum light from the mass donor. Likely this would mean that we only see the shell spectrum from a region that is shadowed from the high flux of the inner disk by the mass donor. The density in this region would have to be high to produce the observed A type spectrum. Moreover, the strength of the lines indicates a stellar flux contribution that matches that expected from the light curve, as shown above. So not only is the light being absorbed continuum light from the star, but the absorption must be occurring over most or all of the stellar disk. This inferred combination of high opacity and full disk coverage suggests that the lines have a photospheric rather than shell origin. Second, the radial velocity variations we observe mean that any “shell” source must also be orbiting within the system near the donor. This is somewhat consistent with the idea of a shadowed region, since the shadow would move with the mass donor. The problem here is that the gas in the shadowed region is unlikely to be gravitationally bound to the donor if the donor fills its Roche lobe. Thus, any “shell” gas component in this location is likely transient and may not produce the Keplerian motion we observe. Third, the  $v_{rot} \sin i$  we measure in the SS 433 spectrum is at the upper end of values for A supergiants. It is doubtful that a shell spectrum in this region would produce  $v_{rot} \sin i$  values this high. One certain constraint we can place in the event of a shell spectrum is that the spectral type of the mass donor must be earlier than A7. Were the mass donor of later spectral type the

dense shell would be hotter than the star, which is very unlikely.

It is interesting to note that Charles et al. (2004) have also obtained blue spectroscopy of SS 433, though at precessional phases when the disk was nearly edge-on. They show features in the same spectral range as our results which also seem to indicate the presence of a late A-type spectrum. However, the velocities that they arrive at using these absorption features are some  $220 \text{ km s}^{-1}$  more negative than ours and do not show Keplerian motion. Charles et al. (2004) do mention that the interpretation of their results will be complicated if the mass donor is embedded in a dense outflowing disk wind (likely occurring in the orbital plane). This reiterates our reasoning for observing at precessional phase zero, when the mass donor would be above such an outflow rather than embedded in it.

Additionally, the absorption features found in the Charles et al. (2004) spectra appear to be quite different than we present here. In addition to the very different radial velocities, the features in their spectra are *much* stronger and broader than those we have observed. The type of absorption they observe was also discussed by Margon (1984). He explains this absorption as a shell spectrum and notes that the strength of the lines depends strongly on the precessional phase, with the strongest lines appearing when the disk is edge-on. This is precisely when Charles et al. (2004) made their observations. Margon (1984) attributes these lines to the accretion disk. The lines we have observed have very different characteristics. They appear to be much weaker than the lines in Charles et al. (2004), vary through eclipse, have a well-defined Keplerian velocity behavior, and have the relative strength expected for lines from the photosphere of the mass donor star, as described above.

## 6. Conclusion

We have shown that the mass donor in SS 433 is likely to be an A3-7 I star. A similar kind of absorption spectrum may be produced by circumstellar gas, but we argue that the strength of the spectrum and its orbital variation in intensity and Doppler shift all indicate a photospheric origin. Further observations with higher S/N ratio spectra would allow us to classify more accurately the spectrum and calculate temperature, abundances, and surface gravity for the mass donor. With additional radial velocity measurements to help constrain the fit, more accurate masses would also be obtained which would lead to a more secure identification of the compact star as either a black hole or neutron star.

Our estimates of the mass ratio and masses fall within the values predicted in the literature and begin to give us a more definite understanding of the physical parameters of this peculiar system. The evolutionary scenario which best fits our determined physical

parameters is that of King et al. (2000), in which the mass donor star is in a phase of rapid evolution as it crosses the Hertzsprung gap and the compact companion is a low mass black hole.

We have also shown that the orbital ephemeris of Goranskii et al. (1998) and disk precession/nodding model parameters of Gies et al. (2002) are still valid.

We thank the staffs of KPNO and McDonald Observatory for their assistance in making these observations possible. MAS would like to thank T. Bogdanovic for assisting with the observing run. We are grateful to Bruce Margon for comments on an early draft of this work. Financial support was provided by the National Science Foundation through grant AST–0205297 (DRG). Institutional support has been provided from the GSU College of Arts and Sciences and from the Research Program Enhancement fund of the Board of Regents of the University System of Georgia, administered through the GSU Office of the Vice President for Research. Additional funding was provided through a Zaccheus Daniel Foundation Fellowship (MAS).

## REFERENCES

- Antokhina, E. A., & Cherepashchuk, A. M. 1987, *Soviet Astron.*, 31, 295
- Antokhina, E. A., Seifina, E. V., & Cherepashchuk, A. M. 1987, *Soviet Astron.*, 36, 143
- Ballereau, D. 1980, *A&AS*, 41, 305
- Barziv, O., Kaper, L., van Kerkwijk, M. H., Telting, J. H., & van Paradijs, J. 2001, *A&A*, 377, 925
- Berger, D. H., & Gies, D. R. 2001, *ApJ*, 555, 364
- Brandt, N., & Podsiadlowski, Ph. 1995, *MNRAS*, 274, 461
- Collins, G. W., II, & Scher, R. W. 2002, *MNRAS*, 336, 1011
- Charles, P. A., et al. 2004, *RevMexAA(SC)*, in press (astro-ph/0402070)
- Crampton, D., Cowley, A. P., & Hutchings, J. B. 1980, *ApJ*, 235, L131
- Crampton, D., & Hutchings, J. B. 1981, *ApJ*, 251, 604
- D’Odorico, S., Oosterloo, T., Zwitter, T., & Calvani, M. 1991, *Nature*, 353, 329

- Dubner, G. M., Holdaway, M., Goss, W. M., & Mirabel, I. F. 1998, *AJ*, 116, 1842
- Eggleton, P. P. 1983, *ApJ*, 268, 368
- Eikenberry, S. S., Cameron, P. B., Fierce, B. W., Kull, D. M., Dror, D. H., Houck, J. R., & Margon, B. 2001, *ApJ*, 561, 1027
- Fabrika, S. N., & Bychkova, L. V. 1990, *A&A*, 240, L5
- Gies, D. R., Huang, W., & McSwain, M. V. 2003, *ApJ*, 578, L67 (GHM03)
- Gies, D. R., McSwain, M. V., Riddle, R. L., Wang, Z., Wiita, P. J., & Wingert, D. W. 2002, *ApJ*, 566, 1069
- Goranskii, V. P., Esipov, V. F., & Cherepashchuk, A. M. 1998, *Astron. Rep.*, 42, 209
- Goranskii, V. P., Fabrika, S. N., Rakhimov, V. Yu., Panferov, A. A., Belov, A. N., & Bychkova, L. V. 1997, *Astr. Rep.*, 41, 656
- Katz, J. J., Anderson, S. F., Margon, B., & Grandi, S. A. 1982, *ApJ*, 260, 780
- Kemp, J. C., et al. 1986, *ApJ*, 305, 805
- King, A. R., Taam, R. E., & Begelman, M. C. 2000, *ApJ*, 530, L25
- Leibowitz, E. M. 1984, *MNRAS*, 210, 279
- Margon, B. 1982, *Science*, 215, 247
- Margon, B. 1984, *ARA&A*, 22, 507
- Margon, B., & Anderson, S. F. 1989, *ApJ*, 347, 448
- Margon, B., Anderson, S. F., Aller, L. H., Downes, R. A., & Keyes, C. D. 1984, *ApJ*, 281, 313
- Quaintrell, H., et al. 2003, *A&A*, 401, 313
- Stirling, A. M., Jowett, F. H., Spencer, R. E., Paragi, Z., Ogley, R. N., & Cawthorne, T. V. 2002, *MNRAS*, 337, 657
- Thorsett, S. E., & Chakrabarty, D. 1999, *ApJ*, 512, 288
- Venn, K. A. 1995, *ApJS*, 99, 659

Vermeulen, R. C., Schilizzi, R. T., Spencer, R. E., Romney, J. D., & Fejes, I. 1993, *A&A*, 270, 177

Wade, R. A., & Rucinski, S. M. 1985, *A&AS*, 60, 471